

---

# WATT: Weight Average Test-Time Adaption of CLIP

---

David Osowiechi\*

Mehrdad Noori\*

Gustavo A. Vargas Hakim

Moslem Yazdanpanah

Ali Bahri

Milad Cheraghalikhani

Sahar Dastani

Farzad Beizaee

Ismail Ben Ayed

Christian Desrosiers

LIVIA, ÉTS Montréal, Canada  
 International Laboratory on Learning Systems (ILLS),  
 MCGILL - ETS - MILA - CNRS - Université Paris-Saclay - CentraleSupélec, Canada

## Abstract

Vision-Language Models (VLMs) such as CLIP have yielded unprecedented performance for zero-shot image classification, yet their generalization capability may still be seriously challenged when confronted to domain shifts. In response, we present Weight Average Test-Time Adaptation (WATT) of CLIP, a pioneering approach facilitating full test-time adaptation (TTA) of this VLM. Our method employs a diverse set of templates for text prompts, augmenting the existing framework of CLIP. Predictions are utilized as pseudo labels for model updates, followed by weight averaging to consolidate the learned information globally. Furthermore, we introduce a text ensemble strategy, enhancing overall test performance by aggregating diverse textual cues. Our findings underscore the efficacy of WATT in enhancing performance across diverse datasets, including CIFAR-10-C, CIFAR-10.1, CIFAR-100-C, VisDA-C, and several other challenging datasets, effectively covering a wide range of domain shifts. Notably, these enhancements are achieved without necessitating additional model transformations or trainable modules. Moreover, compared to other Test-Time Adaptation methods, our approach can operate effectively with just a single image. Highlighting the potential of innovative test-time strategies, this research emphasizes their role in fortifying the adaptability of VLMs. The implementation is available at: <https://github.com/Mehrdad-Noori/WATT.git>.

## 1 Introduction

The integration of vision and language modalities into a unified learning framework, known as Vision Language models (VLM), has showcased remarkable efficacy in a broad range of vision-related tasks [1, 2, 3]. Notably, these models excel in zero-shot generalization scenarios, where they demonstrate proficiency in tasks beyond their original training scope without requiring additional fine-tuning supervision. Applications of models like CLIP [1] extend across diverse domains including video recognition [4], audio processing [5], and medical imaging [6]. These advancements underscore the pivotal role of such methods in shaping the trajectory of future research and applications in machine learning.

Despite its powerful capabilities, CLIP, like other traditional deep architectures such as Convolutional Neural Networks (CNNs), experiences performance degradation when confronted with domains it

---

\*Equal contribution

	$T^0$	$T^1$	$T^2$	$T^3$	$T^4$	$T^5$	$T^6$	$T^7$	WATT
Original	89.80	90.37	90.50	88.42	89.93	89.95	90.13	88.54	<b>91.05</b>
Gaussian Noise	60.19	61.01	61.17	58.24	58.84	58.35	59.62	61.13	<b>63.84</b>
Defocus Blur	77.23	77.07	78.00	75.98	76.39	77.45	77.08	75.59	<b>78.94</b>
Snow	76.57	77.36	77.93	75.08	77.45	77.09	77.05	75.57	<b>79.79</b>
JPEG Compression	64.65	65.36	65.24	64.16	64.18	64.36	64.78	65.32	<b>67.36</b>

Table 1: Comparison of accuracy (%) using cross-entropy (CE) on CIFAR-10 and some corruptions of CIFAR-10-C datasets on different templates (please see Table 2) and the weight average.

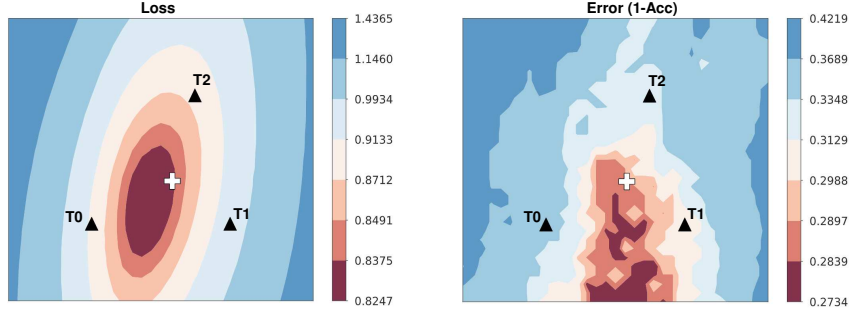


Figure 1: Loss and Error surfaces on model parameters for the Gaussian noise corruption of the CIFAR-10C dataset. Points  $T^0$ ,  $T^1$ , and  $T^2$  represent models adapted with different text templates (please see Table 2). The central point (cross) shows the model obtained by averaging these weights, demonstrating improved performance.

has not been trained on. Current research trends emphasize the importance of domain adaptation mechanisms in the deployment of CLIP [7, 8]. However, a significant challenge remains: swiftly and effectively adapting the model to new domains in real-time while preserving its attractive zero-shot capabilities, thus obviating the need for retraining.

To tackle this challenge, we investigate the impact of different text prompt templates on model adaptation. A key observation driving our approach is the varying performance outcomes yielded by different text prompt templates when used for model adaptation. As shown in Table 1, the classification accuracy obtained with different text prompt templates on some corruptions of the CIFAR-10 dataset fluctuates by up to 3%. Given this insight, finding an effective way to leverage the knowledge from different text templates would be useful to yield a better adaptation. This motivates our work proposing Weight Average adaptation during Test-Time (WATT).

By strategically averaging the adapted weights derived from multiple text prompt templates, our method aims to harness the complementary strengths of individual templates, resulting in robust and enhanced performance across a wide range of domain shifts. To further illustrate this point, Figure 1 presents the test loss and adaptation error surfaces for three models that are separately adapted using three templates ( $T^0$ ,  $T^1$ ,  $T^2$ ) under the Gaussian noise corruption of the CIFAR-10-C dataset<sup>2</sup>. The central point in these landscapes, representing the final model obtained by averaging the weights of the separate models, demonstrates a convergence towards lower loss and error, highlighting the potential of weight averaging for test-time adaptation. Moreover, inspired by recent advancements in machine learning utilizing train-time weight averaging techniques [10, 11], the proposed WATT method can dynamically adjust to new data to tackle unforeseen distribution shifts without relying on class supervision.

We outline the main contributions of our work as follows:

- We introduce a novel Test-Time Adaptation method for CLIP that, for the first time, leverages weight averaging across various text templates at test-time.

<sup>2</sup>To visualize the loss and error surface, we use weight vectors from models adapted with text templates  $T^0$ ,  $T^1$ , and  $T^2$ , denoted as  $w_0$ ,  $w_1$ , and  $w_2$ . Following [9], we define  $u = w_1 - w_0$  and  $v = (w_2 - w_0) - \frac{(w_2 - w_0) \cdot (w_1 - w_0)}{\|w_1 - w_0\|^2} (w_1 - w_0)$ . The normalized vectors  $\hat{u} = \frac{u}{\|u\|}$  and  $\hat{v} = \frac{v}{\|v\|}$  form an orthonormal basis in the plane of  $w_0$ ,  $w_1$ , and  $w_2$ . We create a Cartesian grid in this basis and evaluate the networks at each grid point. A point  $P$  with coordinates  $(x, y)$  in the plane is given by  $P = w_0 + x \cdot \hat{u} + y \cdot \hat{v}$ . To plot all in the same plane, we used the average of the three templates’ text embeddings.

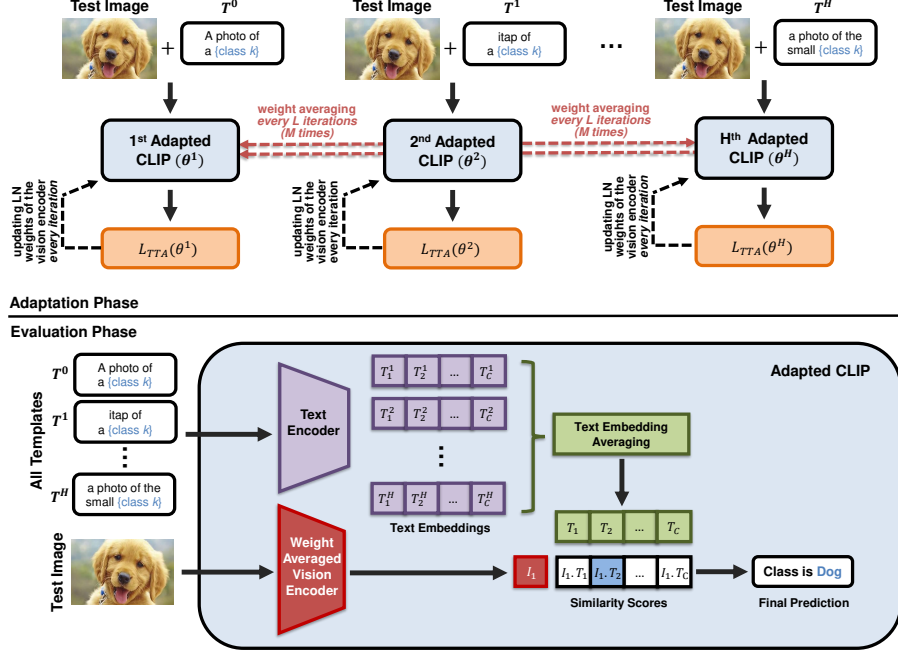


Figure 2: Overview of the proposed WATT method. In the Adaptation Phase, the model is adapted using different text templates ( $T^0, T^1, \dots, T^H$ ), with weight averaging performed periodically. In the Evaluation Phase, the adapted CLIP model uses averaged text embeddings from all templates and the weight averaged model to predict the class of the test image.

- Our WATT method represents a pioneering advancement within the TTA paradigm, achieving exceptional performance with the ability to improve using only a single image at test time, a capability not present in previous approaches.
- We rigorously evaluate our WATT methodology through comprehensive evaluations across different datasets characterized by diverse types and degrees of domain shifts, encompassing **a total of 155 evaluation scenarios**. Our experiments demonstrate the robustness and efficacy of WATT compared to existing adaptation methods.

## 2 Related work

**Test-Time Adaptation (TTA)** is crucial in domain adaptation, particularly with unlabeled target domain data and no access to source domain samples. The challenge lies in estimating the target domain’s distribution and comparing domain characteristics indirectly. Recent advancements have highlighted the potential and limitations of adapting pre-trained models. A key focus has been on leveraging batch normalization layers for adaptation due to their ability to retain source domain information. Methods such as PTBN [12] and TENT [13] recalibrate batch statistics and optimize affine parameters via entropy minimization, though they often require image augmentations or large batches. LAME [14] introduces a closed-form optimization strategy that refines model predictions for target images by leveraging the Laplacian of feature maps to encourage clustering, thereby emphasizing feature similarities.

Recently, Test-Time Training (TTT) methodologies have emerged as prominent contenders in TTA [15, 16, 17, 18, 19]. This approach involves training a supplementary sub-branch alongside the primary network in an unsupervised manner, subsequently leveraging it to refine the model. Unlike previous methods, our approach operates on individual image batches, offering a significant advantage in TTA by avoiding the necessity of training additional branches from scratch.

In natural language processing, TPT [8] introduced entropy minimization for adapting models like CLIP, albeit with high computational costs due to learning an adapter at the text prompt with multiple transformations. CLIPArTT [20], in contrast, fine-tunes normalization layers with minimal disruption to the model’s knowledge, enhancing text supervision by introducing pseudo-labels. Existing methods often lag behind supervised prompt adaptation techniques in performance. SwapPrompt [21] bridges

this gap by leveraging self-supervised contrastive learning, employing a dual prompts paradigm. Our method combines prompt augmentation and fine-tuning of normalization layers, highlighting its effectiveness in test-time adaptation.

**Weight Averaging (WA)** is a powerful train-time technique for improving deep neural network generalization. Stochastic Weight Averaging (SWA) [22] averages weights of multiple models sampled from different training epochs, aiding smooth optimization trajectory and convergence to points with superior generalization. SWAD [10] refines SWA by densely sampling weights throughout training, enhancing generalization and robustness across tasks. This train-time refinement enhances WA’s effectiveness in producing models with improved generalization. The Lookaround [11] optimizer iterates between an “around step” and an “average step”, building on SWAD’s advancements. In the “around step”, independently trained models using various data augmentations explore a broader loss landscape to find flatter minima. In the “average step”, weights of these models are then averaged, guiding optimization towards lower loss regions. This method enhances robustness and generalization across tasks, improving upon SWA and SWAD by providing a more effective weight averaging process.

In contrast to existing approaches, WATT leverages varied text prompts to adapt vision-language models such as CLIP during testing. Our method also harnesses the benefits of weight averaging while addressing domain shifts without additional model transformations or trainable modules, thereby setting a new precedent in test-time adaptation.

### 3 Method

The proposed WATT method, summarized visually in Figure 2 comprises three main components, the first two in the Adaptation Phase and the third in the Evaluation Phase: **1)** a light-weight transductive TTA strategy that adapts CLIP’s visual encoder efficiently by considering the similarity between *all* batch samples in terms of their visual and text features; **2)** a weight-averaging strategy using multiple text templates to generate diverse model hypotheses during adaptation; **3)** an ensembling technique that boosts performance during evaluation by averaging the embedding of different text templates.

#### 3.1 Transductive TTA loss

While our method can be employed with any TTA framework, in this work, we implement a strategy inspired by the transductive TTA approach of CLIPArTT [20] which effectively incorporates semantic relationships among batch samples.

Initially, our process involves executing inference using CLIP, a system comprising a visual encoder  $f_{\theta}^v(\cdot)$  that translates an image  $\mathbf{x}$  into visual features  $\mathbf{z}^v \in \mathbb{R}^D$ , and a text encoder  $f_{\theta}^t(\cdot)$  which converts text prompts  $\mathbf{t}$  into text features  $\mathbf{z}^t \in \mathbb{R}^D$ . During inference, we employ pre-defined text prompts assigned to each class within a dataset, such as  $\mathbf{t}_k^0 = \text{“a photo of a \{class } k\text{”}$ . For a new image  $\mathbf{x}_i$ , the likelihood of belonging to class  $k$  is then computed using cosine similarity:

$$p_{ik} = \frac{\exp(\cos(\mathbf{z}_i^v, \mathbf{z}_k^t)/\tau)}{\sum_j \exp(\cos(\mathbf{z}_i^v, \mathbf{z}_j^t)/\tau)}, \quad \cos(\mathbf{z}, \mathbf{z}') = \frac{\mathbf{z}^\top \mathbf{z}'}{\|\mathbf{z}\|_2 \cdot \|\mathbf{z}'\|_2}, \quad (1)$$

where  $\tau$  is a softmax temperature parameter set to 0.01 in this work. This prediction is then stored to be used as pseudo-labels for the model.

Denoting the normalized visual embeddings of the samples within the test batch as  $\mathbf{Z}^v \in \mathbb{R}^{B \times D}$  and the instance-specific text embeddings as  $\mathbf{Z}^t \in \mathbb{R}^{B \times D}$ , we compute an image-to-image similarity matrix  $\mathbf{S}^v = \mathbf{Z}^v (\mathbf{Z}^v)^\top \in [-1, 1]^{B \times B}$  modeling pairwise relationships in terms of image characteristics. Similarly, we construct a text-to-text similarity matrix  $\mathbf{S}^t = \mathbf{Z}^t (\mathbf{Z}^t)^\top \in [-1, 1]^{B \times B}$ , capturing the semantic relationships among text embeddings within the batch. Utilizing the computed pairwise similarity matrices, we generate pseudo-labels  $\mathbf{Q} = \text{softmax}((\mathbf{S}^v + \mathbf{S}^t)/2\tau) \in [0, 1]^{B \times B}$  which are used with cross-entropy in our transductive TTA loss:

$$\mathcal{L}_{\text{TTA}}(\theta) = -\frac{1}{B} \sum_{i=1}^B \sum_{j=1}^B q_{ij} \log p_{ij}. \quad (2)$$

Template
$T^0$ : “a photo of a {class $k$ }”
$T^1$ : “itap of a {class $k$ }”
$T^2$ : “a bad photo of the {class $k$ }”
$T^3$ : “a origami {class $k$ }”
$T^4$ : “a photo of the large {class $k$ }”
$T^5$ : “a {class $k$ } in a video game”
$T^6$ : “art of the {class $k$ }”
$T^7$ : “a photo of the small {class $k$ }”

Table 2: The different templates used during the experiments.

Dataset	single_temp	text_avg
CIFAR-10	$90.87 \pm 0.10$	<b><math>91.08 \pm 0.06</math></b>
CIFAR-10.1	$86.80 \pm 0.19$	<b><math>86.85 \pm 0.18</math></b>
CIFAR-10-C	72.08	<b>72.66</b>
CIFAR-100	$69.79 \pm 0.20$	<b><math>70.30 \pm 0.11</math></b>
CIFAR-100-C	41.79	<b>42.24</b>

Table 3: Accuracy (%) with different text ensembles at test time.

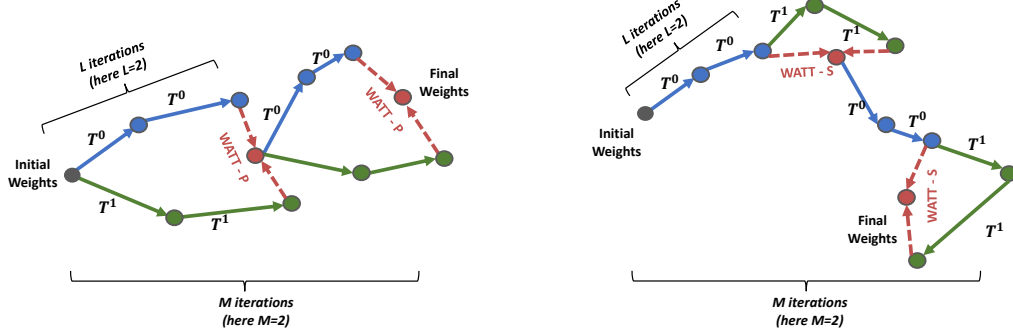


Figure 3: Visual comparison of the Parallel (**left**) and Sequential (**right**) approaches for multi-template weight averaging during adaptation.

Drawing a link with the Stochastic Neighbor Embedding (SNE) method for dimensionality reduction [23], which minimizes the KL divergence between distributions modeling pairwise distances, our TTA loss ensures that the inter-modality (text-to-image) similarities of batch samples are aligned with their intra-modality ones (text-to-text and image-to-image).

### 3.2 Multi-Template Weight Averaging

We explore various text prompt templates suggested in the CLIP paper and detailed in Table 2. As reported in Table 1, these prompts achieve varying performance across different corruption types of CIFAR-10-C. We formulate prompts of the form  $t_k^h = \text{template } h(\text{class } k)$ , where  $h \in \{1, 2, \dots, H\}$ , encompassing a spectrum of textual cues tailored to elicit diverse responses from the model.

Two different approaches are investigated for our multi-template weight averaging (MTWA) strategy. The first one denoted as **Parallel MTWA (WATT-P)**, which follows recent optimization approaches like Lookaround [11], performs the adaptation separately for each text template, starting from the same parameters, and then averages the resulting adapted weights. The second one, called **Sequential MTWA (WATT-S)**, instead considers text templates sequentially without resetting the weights. These two approaches, which we illustrate and compare in Fig. 3, are detailed below.

**Parallel MTWA.** This approach optimizes the TTA loss in (2) separately for  $H$  different models, each utilizing a distinct template. Starting from the same visual encoder parameters  $\theta$ , these models are updated in parallel for  $L$  iterations, resulting in updated parameters  $\theta'_h$ , with  $h \in \{1, \dots, H\}$ . The parameters are reset after each update, enabling each model to restart the adaptation from the same initial point. Subsequently, we aggregate the weights obtained from these  $H$  models by computing their average:  $\theta_{\text{avg}} = \frac{1}{H} \sum_{h=1}^H \theta'_h$ . We repeat this step  $M$  times, and denote the overall process as “(after  $L$  iter)  $\times M$ ”.

**Sequential MTWA.** Our Sequential MTWA approach is inspired from the work of [22], where the averaging of weights across various stages of the training process is employed to mitigate variance and enhance generalization capabilities. Instead of resetting parameters for each model, we update

Dataset	CLIP	BS=1	BS=2	BS=4	BS=8	BS=16	BS=32	BS=64	BS=128
CIFAR-10	88.74	89.87	89.39 $\pm 0.02$	89.16 $\pm 0.07$	88.93 $\pm 0.16$	89.14 $\pm 0.04$	89.51 $\pm 0.12$	90.16 $\pm 0.13$	91.05 $\pm 0.06$
CIFAR-10.1	83.25	84.55	84.32 $\pm 0.15$	83.88 $\pm 0.17$	84.12 $\pm 0.37$	84.35 $\pm 0.21$	84.87 $\pm 0.16$	85.52 $\pm 0.30$	86.98 $\pm 0.31$
CIFAR-10-C	59.22	61.26	63.60	63.47	63.94	65.66	68.34	71.21	73.82

Table 4: Accuracy (%) of our method for different batch sizes compared to CLIP.

parameters after each template’s iteration. To ensure impartiality in the update sequence of templates, a random selection process is implemented, thereby disregarding any predetermined order.

### 3.3 Evaluation Phase

At test-time, predictions are computed using Equation 1 through two distinct methodologies. In the first approach, the text features  $\mathbf{z}_0^t$  are derived from the initial text prompt  $\mathbf{t}_k^0 = \text{“a photo of a class } k\text{”}$ , denoted as `single_temp`. Conversely, the second method aggregates the text features from all templates by computing their mean, resulting in the prediction  $\mathbf{z}_{\text{ens}}^t = \frac{1}{H} \sum_{h=1}^H \mathbf{z}_h^t$ , denoted as `text_avg` (see Fig. 2).

## 4 Experimental Setup

**Settings.** In line with prior TTA methodologies, adjustments are made to all Layer Normalization layers within the visual feature extractor for test-time adaptation. The Adam optimizer is employed with a fixed learning rate of  $10^{-3}$ , whereas a smaller learning rate of  $10^{-4}$  is chosen for adaptation to the 3D renderings split, as it reflects a more pronounced shift. Throughout our experimentation process, a consistent batch size of 128 is maintained to ensure uniformity and facilitate meaningful comparisons across various scenarios.

**Datasets.** Following [20], we rigorously evaluate WATT’s performance across diverse TTA datasets using established assessment techniques. These datasets simulate intricate domain shifts, providing nuanced insights into our approach’s effectiveness. Additionally, we explore WATT’s adaptability on the original dataset through zero-shot test-time adaptation. To ensure a thorough examination, we extend our analysis to include various domain generalization datasets, exposing our method to a broad spectrum of image categories for comprehensive evaluation. Our evaluation framework encompasses *natural images*, *common corruptions*, *simulated shifts*, *video shifts*, *texture shifts* and *style shifts*.

In our assessment of natural image analysis, we include CIFAR-10, CIFAR-10.1, and CIFAR-100, each comprising 10,000 images and offering varied data distributions. CIFAR-10.1 [24] introduces a natural shift from CIFAR-10, providing a comprehensive evaluation of our model’s performance. We also incorporate the CIFAR-10-C and CIFAR-100-C datasets [24], augmented with 15 distinct corruptions across 5 severity levels, resulting in 75 common corruption scenarios. This comprehensive augmentation assesses the model’s resilience effectively.

Our investigation also extends to the VisDA-C dataset [25], challenging models with simulated and video shifts across diverse imagery types. Additionally, we evaluate our method on three datasets mostly used in the field of domain generalization: PACS [26], VLCS [27], and OfficeHome [28] datasets, instrumental in understanding texture and style variations. These evaluations effectively demonstrate the generalizability of our method across distinct domain shifts.

**Benchmarking.** We conduct a comparative analysis of WATT against contemporary methodologies using ViT-B/32 as backbone. Specifically, we incorporate an adapted version of TENT [13], customized for CLIP by the authors of [20], with 10 iterations. We also compare with TPT [8], a novel adaptation technique for CLIP, which heavily relies on image augmentations. Due to its demanding memory requirements, we decrease the batch size to 32. Lastly, we include CLIPArTT [20], a recent approach utilizing pseudo labels generated through conformal learning methodologies.

## 5 Results

In this section, we present empirical findings from our WATT method through a series of ablation studies aimed at understanding the impacts of individual components. These studies inform subsequent

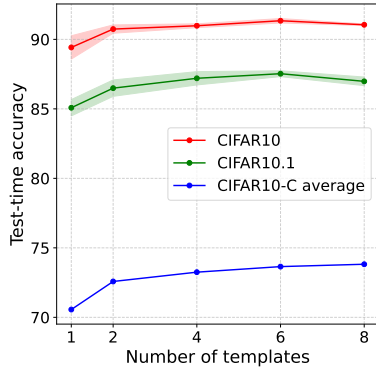


Figure 4: Evolution of the accuracy for different numbers of random template on 5 test-time runs.

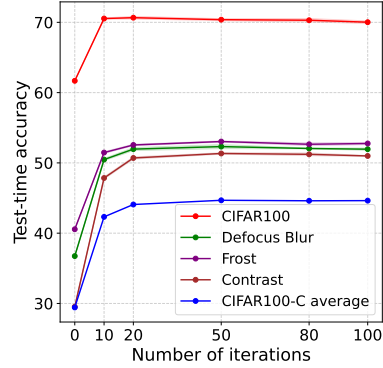


Figure 5: Evolution of accuracy on CIFAR-100 corruptions with the Parallel MTWA method.

experiments across diverse datasets. Leveraging insights from ablations, we conduct comprehensive experiments, benchmarking WATT against state-of-the-art techniques across various datasets.

### 5.1 Ablation Studies

In this section, unless otherwise specified, we focus on the Sequential MTWA variant of our method (see Section 3.2) and will use these findings as a reference for the Parallel MTWA method.

**Comparison of the template used during testing.** After updating the model, we proceed to compute the similarity between the image features and the text embeddings, enabling prediction. Typically, text embeddings originate from the text prompt “a photo of a class  $k$ ”. However, by employing multiple templates, we have the flexibility to alter this text embedding through the averaging of all text embeddings from each template. Table 3 conducts a comparative analysis revealing that this averaged text embedding consistently yields superior results across all scenarios. Hence, we adopt this approach for next experiments.

**Comparison of the number of templates.** In Figure 4, we examine the performance variation relative to the number of utilized templates. In this investigation, we conduct 5 runs wherein the templates are randomly selected from a pool of 8 distinct templates (as outlined in Table 2). Notably, when the distribution shift is minimal, as observed in CIFAR-10 and CIFAR-10.1, optimal performance is attained using 6 templates, with performance gradually diminishing thereafter. Conversely, in scenarios characterized by substantial corruptions, such as CIFAR-10-C, employing all 8 templates proves advantageous. Consequently, our focus moving forward will be on utilizing all 8 templates in our work.

Dataset	Text avg.	Output avg.	Weight avg. (ours)		
			(after 10 iter)×1	(after 1 iter)×10	(after 2 iter)×5
CIFAR-10	90.58 ±0.03	90.90 ±0.03	91.08 ±0.06	<b>91.39 ±0.14</b>	91.05 ±0.06
CIFAR-10.1	85.78 ±0.25	86.77 ±0.08	86.85 ±0.18	<b>88.02 ±0.18</b>	86.98 ±0.31
CIFAR-10-C	71.41	72.60	72.66	73.66	<b>73.82</b>
CIFAR-100	69.46 ±0.13	70.32 ±0.1	70.3 ±0.11	<b>70.85 ±0.08</b>	70.74 ±0.20
CIFAR-100-C	41.37	42.68	42.24	45.32	<b>45.57</b>

Table 5: Accuracy (%) obtained with different averaging strategies.

**Text Averaging vs Output Averaging vs Weight Averaging.** Utilizing the averaging method within a VLM offers several possibilities, including averaging the weights, the outputs or the text embeddings before computing the logits. In Table 5, a comparison between these approaches is presented. It becomes evident that weight averaging consistently outperforms text embedding averaging across various datasets, showcasing a superiority of approximately 1% even with the less effective weight

Dataset	CLIP	TENT	TPT (BS=32)	CLIPArTT	WATT-P	WATT-S	
CIFAR-10	88.74	<b>91.69</b> $\pm 0.10$	88.06 $\pm 0.06$	90.04 $\pm 0.13$	91.41 $\pm 0.17$	91.05 $\pm 0.06$	
CIFAR-10.1	83.25	87.60 $\pm 0.45$	81.80 $\pm 0.27$	86.35 $\pm 0.27$	<b>87.78</b> $\pm 0.05$	86.98 $\pm 0.31$	
CIFAR-10-C	59.22	67.56	56.80	71.17	72.83	<b>73.82</b>	
CIFAR-100	61.68	69.74 $\pm 0.16$	63.78 $\pm 0.28$	69.79 $\pm 0.04$	70.38 $\pm 0.14$	<b>70.74</b> $\pm 0.20$	
CIFAR-100-C	Gaussian Noise	14.80	14.38 $\pm 0.14$	14.03 $\pm 0.10$	25.32 $\pm 0.14$	31.28 $\pm 0.03$	<b>32.07</b> $\pm 0.23$
	Shot noise	16.03	17.34 $\pm 0.27$	15.25 $\pm 0.17$	27.90 $\pm 0.05$	33.44 $\pm 0.11$	<b>34.36</b> $\pm 0.11$
	Impulse Noise	13.85	10.03 $\pm 0.13$	13.01 $\pm 0.13$	25.62 $\pm 0.09$	29.40 $\pm 0.11$	<b>30.33</b> $\pm 0.03$
	Defocus blur	36.74	49.05 $\pm 0.07$	37.60 $\pm 0.17$	49.88 $\pm 0.23$	52.32 $\pm 0.28$	<b>52.99</b> $\pm 0.16$
	Glass blur	14.19	3.71 $\pm 0.07$	16.41 $\pm 0.02$	27.89 $\pm 0.03$	31.20 $\pm 0.12$	<b>32.15</b> $\pm 0.30$
	Motion blur	36.14	46.62 $\pm 0.27$	37.52 $\pm 0.23$	47.93 $\pm 0.14$	49.72 $\pm 0.15$	<b>50.53</b> $\pm 0.12$
	Zoom blur	40.24	51.84 $\pm 0.15$	42.99 $\pm 0.11$	52.70 $\pm 0.06$	54.72 $\pm 0.04$	<b>55.30</b> $\pm 0.22$
	Snow	38.95	46.71 $\pm 0.21$	42.35 $\pm 0.13$	49.72 $\pm 0.01$	51.79 $\pm 0.04$	<b>52.77</b> $\pm 0.15$
	Frost	40.56	44.90 $\pm 0.27$	43.31 $\pm 0.14$	49.63 $\pm 0.12$	53.04 $\pm 0.08$	<b>53.79</b> $\pm 0.31$
	Fog	38.00	47.31 $\pm 0.04$	38.81 $\pm 0.17$	48.77 $\pm 0.04$	50.78 $\pm 0.24$	<b>51.49</b> $\pm 0.21$
	Brightness	48.18	60.58 $\pm 0.18$	50.23 $\pm 0.11$	61.27 $\pm 0.08$	62.65 $\pm 0.25$	<b>63.57</b> $\pm 0.21$
	Contrast	29.53	45.90 $\pm 0.11$	28.09 $\pm 0.09$	48.55 $\pm 0.24$	51.34 $\pm 0.10$	<b>52.76</b> $\pm 0.27$
	Elastic transform	26.33	33.09 $\pm 0.08$	28.12 $\pm 0.15$	37.45 $\pm 0.08$	39.97 $\pm 0.06$	<b>40.90</b> $\pm 0.43$
	Pixelate	21.98	26.47 $\pm 0.09$	20.43 $\pm 0.14$	33.88 $\pm 0.14$	39.59 $\pm 0.09$	<b>40.97</b> $\pm 0.16$
	JPEG compression	25.91	29.89 $\pm 0.07$	28.82 $\pm 0.09$	36.07 $\pm 0.32$	38.99 $\pm 0.16$	<b>39.59</b> $\pm 0.08$
Mean	29.43	35.19	30.46	41.51	44.68	<b>45.57</b>	

Table 6: Accuracy (%) on CIFAR-10, CIFAR-10.1, CIFAR-10-C, CIFAR-100 and CIFAR-100-C datasets. WATT-P refers to our method with Parallel MTWA and WATT-S to the Sequential MTWA variant of WATT.

averaging method. This performance advantage is observed across CIFAR-10, CIFAR-10.1, and CIFAR-10-C, and persists even with larger numbers of classes, such as in CIFAR-100 and CIFAR-100-C. When concentrating on output averaging, the results may be less evident with less effective weight averaging methods. However, they remain valid and even more accurate with superior weight averaging techniques. Therefore, our focus for future experiments will be on weight averaging as the preferred approach.

**Best moment to do the Weight Averaging.** Examining Table 5, it is evident that the parameters  $L$  and  $M$  discussed in Section 3 are crucial. Specifically, a large  $L$  (e.g., 10) combined with a small  $M$  (e.g., 1) is ineffective. Conversely, setting  $L = 1$  and  $M = 10$  yields optimal results for small distribution shift datasets, while  $L = 2$  and  $M = 5$  perform best on highly corrupted datasets. Given that TTA typically encounters substantial distribution shifts, we will use  $L = 2$  and  $M = 5$  in our subsequent experiments.

**Performance over the number of iterations.** In this section, we focus on the method incorporating a Parallel MTWA mechanism and examine the impact of the number of iterations on performance. As illustrated in Figure 5, the accuracy stabilizes after approximately 20 iterations. Although there is a slight improvement in performance beyond 50 iterations, the difference is marginal. Based on these observations, we have opted to use 50 iterations for our experiments.

**Model performance across various batch sizes.** In our investigation, we delve into the performance implications of TTA methods when operating under small batch sizes, a historical challenge in the field. Table 4 provides insights into this aspect, revealing substantial performance enhancements with increasing batch sizes. Notably, our WATT model showcases remarkable adaptability, demonstrating performance improvements even with a single image input contrary to alternative methods. Specifically, we observe enhancements of approximately 1% for CIFAR-10 and CIFAR-10.1, and an impressive 2% for CIFAR-10-C when compared to baseline. Moving forward, we maintain a batch size of 128 in our experiments, aligning with prevalent practices observed in contemporary state-of-the-art methodologies.



Dataset	Domain	CLIP	TENT	TPT	CLIPArTT	WATT-P	WATT-S
VisDA-C	3D (trainset)	84.43	84.86 $\pm 0.01$	79.35 $\pm 0.04$	85.09 $\pm 0.01$	<b>85.42 <math>\pm 0.03</math></b>	85.36 $\pm 0.01$
	YT (valset)	84.45	84.68 $\pm 0.01$	83.57 $\pm 0.04$	84.40 $\pm 0.01$	84.57 $\pm 0.00$	<b>84.69 <math>\pm 0.01</math></b>
	Mean	84.44	84.77	81.46	84.75	85.00	<b>85.03</b>
OfficeHome	Art	73.75	74.03 $\pm 0.27$	<b>75.76 <math>\pm 0.27</math></b>	73.84 $\pm 0.20$	75.65 $\pm 0.27$	<b>75.76 <math>\pm 0.39</math></b>
	Clipart	63.33	63.42 $\pm 0.04$	63.08 $\pm 0.31$	63.54 $\pm 0.06$	<b>66.23 <math>\pm 0.13</math></b>	65.77 $\pm 0.11$
	Product	85.32	<b>85.51 <math>\pm 0.08</math></b>	84.07 $\pm 0.28$	85.23 $\pm 0.16$	85.41 $\pm 0.09$	85.41 $\pm 0.01$
	Real World	87.71	87.74 $\pm 0.05$	85.89 $\pm 0.33$	87.61 $\pm 0.05$	88.22 $\pm 0.15$	<b>88.37 <math>\pm 0.05</math></b>
	Mean	77.53	77.68	77.20	77.56	<b>78.88</b>	78.83
PACS	Art	96.34	<b>96.65 <math>\pm 0.05</math></b>	95.52 $\pm 0.20$	96.57 $\pm 0.09$	96.31 $\pm 0.00$	96.39 $\pm 0.00$
	Cartoon	96.08	96.22 $\pm 0.05$	94.77 $\pm 0.20$	96.00 $\pm 0.02$	96.52 $\pm 0.02$	<b>96.62 <math>\pm 0.02</math></b>
	Photo	99.34	99.40 $\pm 0.00$	99.42 $\pm 0.06$	99.28 $\pm 0.00$	99.48 $\pm 0.03$	<b>99.52 <math>\pm 0.00</math></b>
	Sketch	82.85	82.96 $\pm 0.12$	83.22 $\pm 0.14$	83.93 $\pm 0.14$	<b>86.92 <math>\pm 0.04</math></b>	86.65 $\pm 0.12$
	Mean	93.65	93.81	93.23	93.95	<b>94.81</b>	94.80
VLCS	Caltech101	<b>99.51</b>	<b>99.51 <math>\pm 0.00</math></b>	99.36 $\pm 0.06$	<b>99.51 <math>\pm 0.00</math></b>	99.43 $\pm 0.00$	<b>99.51 <math>\pm 0.00</math></b>
	LabelMe	68.15	67.89 $\pm 0.13$	54.88 $\pm 0.12$	67.96 $\pm 0.04$	66.67 $\pm 0.21$	<b>68.49 <math>\pm 0.12</math></b>
	SUN09	68.85	69.27 $\pm 0.04$	67.30 $\pm 0.49$	68.68 $\pm 0.09$	72.61 $\pm 0.15$	<b>73.13 <math>\pm 0.17</math></b>
	VOC2007	84.13	<b>84.42 <math>\pm 0.15</math></b>	76.74 $\pm 0.28$	84.09 $\pm 0.02$	82.30 $\pm 0.16$	83.41 $\pm 0.17$
	Mean	80.16	80.27	74.57	80.06	80.25	<b>81.14</b>

Table 7: Accuracy (%) on different domains of VisDA-C, OfficeHome, PACS and VLCS datasets.

## 5.2 Comparison to SOTA methods

**Performance Evaluation in the Presence of Natural or No Domain Shift** In Table 6, results show consistent performance enhancements with WATT, both with the Parallel and Sequential MTWA strategies, alongside the baseline. On CIFAR-10, performance improves by 2.67% with Parallel MTWA and 2.31% using Sequential MTWA. On CIFAR-10.1, improvements reach 4.53% and 3.73%, and on CIFAR-100, enhancements are 8.70% and 9.06%. While WATT consistently outperforms the baseline, TPT, and CLIPArTT, TENT yields superior results on CIFAR-10. WATT’s effectiveness often correlates with the number of classes, showing better performance with more classes, indicating its strength in lower-confidence scenarios.

**Performance Evaluation in the Presence of Common Corruptions** Table 6 shows that both WATT variants consistently outperform alternative methods across various corruptions and class numbers. Notably, WATT with Parallel MTWA improves performance by 16.48% on CIFAR-100 *Gaussian Noise* and by 17.01% on *Glass Blur* compared to the baseline, while WATT with Sequential MTWA shows improvements of 17.27% and 17.96% respectively. On common corruptions, the Sequential MTWA variant surpasses Parallel MTWA, with improvements of 0.99% on CIFAR-10 and 0.89% on CIFAR-100.

**Performance analysis under simulated and video shifts** Results on the 3D (simulated shift) and YT (video shift) splits of VisDA-C demonstrate a significant improvement in accuracy with our proposed WATT method compared to pure CLIP. The Sequential MTWA variant achieves the highest accuracy on both the 3D and YT splits, with scores of 85.36% and 84.69%, respectively, surpassing other adaptation methods including TENT, TPT, and CLIPArTT (see Table 7).

**Performance analysis under texture and style shifts** Results on the OfficeHome, PACS, and VLCS datasets are presented in Table 7. On average, our proposed WATT method, with Parallel and Sequential MTWA variants, improves performance across the different domains of OfficeHome, PACS, and VLCS compared to other methods. This highlights its robustness in addressing texture and style shifts, which are especially challenging compared to other domain shift variants.

## 6 Conclusion

We introduce WATT, a Test-Time Adaptation method tailored for Vision-Language Models. Our approach harnesses Weight Averaging with different text prompts and incorporates text embeddings averaging to bolster prediction accuracy.

Through an extensive ablation study, we scrutinized the efficacy of employing varied text prompts and weight averaging. Comparative evaluations across Test-Time Adaptation and Domain Generalization datasets underscored the superiority of our method, particularly in scenarios involving distribution shifts and zero-shot performance enhancements compared to state-of-the-art approaches.

Looking forward, investigating the potential of text prompts and weight averaging in classification opens up promising avenues for future exploration. Our methodology, with its focus on template manipulation, suggests potential avenues for extension, such as incorporating alternative class descriptors, yielding valuable insights for future research. Moreover, expanding Test-Time Adaptation to encompass diverse scenarios, including segmentation or object detection with Vision-Language Models, holds significant potential for advancing our comprehension of model adaptability and performance across varied tasks.

## References

- [1] Alec Radford, Jong Wook Kim, Chris Hallacy, Aditya Ramesh, Gabriel Goh, Sandhini Agarwal, Girish Sastry, Amanda Askell, Pamela Mishkin, Jack Clark, et al. Learning transferable visual models from natural language supervision. In *International conference on machine learning*, pages 8748–8763. PMLR, 2021.
- [2] Chao Jia, Yinfei Yang, Ye Xia, Yi-Ting Chen, Zarana Parekh, Hieu Pham, Quoc Le, Yun-Hsuan Sung, Zhen Li, and Tom Duerig. Scaling up visual and vision-language representation learning with noisy text supervision. In *International conference on machine learning*, pages 4904–4916. PMLR, 2021.
- [3] Alexander Kirillov, Eric Mintun, Nikhila Ravi, Hanzi Mao, Chloe Rolland, Laura Gustafson, Tete Xiao, Spencer Whitehead, Alexander C Berg, Wan-Yen Lo, et al. Segment anything. *arXiv preprint arXiv:2304.02643*, 2023.
- [4] Ziyi Lin, Shijie Geng, Renrui Zhang, Peng Gao, Gerard de Melo, Xiaogang Wang, Jifeng Dai, Yu Qiao, and Hongsheng Li. Frozen clip models are efficient video learners. In *European Conference on Computer Vision*, pages 388–404. Springer, 2022.
- [5] Andrey Guzhov, Federico Raue, Jörn Hees, and Andreas Dengel. Audioclip: Extending clip to image, text and audio. In *ICASSP 2022-2022 IEEE International Conference on Acoustics, Speech and Signal Processing (ICASSP)*, pages 976–980. IEEE, 2022.
- [6] Jie Liu, Yixiao Zhang, Jie-Neng Chen, Junfei Xiao, Yongyi Lu, Bennett A Landman, Yixuan Yuan, Alan Yuille, Yucheng Tang, and Zongwei Zhou. Clip-driven universal model for organ segmentation and tumor detection. In *Proceedings of the IEEE/CVF International Conference on Computer Vision*, pages 21152–21164, 2023.
- [7] Zhengfeng Lai, Noranart Vesdapunt, Ning Zhou, Jun Wu, Cong Phuoc Huynh, Xuelu Li, Kah Kuen Fu, and Chen-Nee Chuah. Padclip: Pseudo-labeling with adaptive debiasing in clip for unsupervised domain adaptation. In *Proceedings of the IEEE/CVF International Conference on Computer Vision (ICCV)*, pages 16155–16165, October 2023.
- [8] Manli Shu, Weili Nie, De-An Huang, Zhiding Yu, Tom Goldstein, Anima Anandkumar, and Chaowei Xiao. Test-time prompt tuning for zero-shot generalization in vision-language models. In S. Koyejo, S. Mohamed, A. Agarwal, D. Belgrave, K. Cho, and A. Oh, editors, *Advances in Neural Information Processing Systems*, volume 35, pages 14274–14289. Curran Associates, Inc., 2022.
- [9] Timur Garipov, Pavel Izmailov, Dmitrii Podoprikin, Dmitry P Vetrov, and Andrew G Wilson. Loss surfaces, mode connectivity, and fast ensembling of dnns. In S. Bengio, H. Wallach, H. Larochelle, K. Grauman, N. Cesa-Bianchi, and R. Garnett, editors, *Advances in Neural Information Processing Systems*, volume 31. Curran Associates, Inc., 2018.
- [10] Junbum Cha, Sanghyuk Chun, Kyungjae Lee, Han-Cheol Cho, Seunghyun Park, Yunsung Lee, and Sungrae Park. Swad: Domain generalization by seeking flat minima. *Advances in Neural Information Processing Systems*, 34:22405–22418, 2021.
- [11] Jiangtao Zhang, Shunyu Liu, Jie Song, Tongtian Zhu, Zhengqi Xu, and Mingli Song. Lookaround optimizer:  $k$  steps around, 1 step average. *Advances in Neural Information Processing Systems*, 36, 2024.

- [12] Zachary Nado, Shreyas Padhy, D. Sculley, Alexander D’Amour, Balaji Lakshminarayanan, and Jasper Snoek. Evaluating prediction-time batch normalization for robustness under covariate shift. *arXiv:2006.10963 [cs, stat]*, January 2021. arXiv: 2006.10963.
- [13] Dequan Wang, Evan Shelhamer, Shaoteng Liu, Bruno Olshausen, and Trevor Darrell. Tent: Fully test-time adaptation by entropy minimization. *arXiv preprint arXiv:2006.10726*, 2020.
- [14] Malik Boudiaf, Romain Mueller, Ismail Ben Ayed, and Luca Bertinetto. Parameter-free online test-time adaptation. In *IEEE/CVF Conference on Computer Vision and Pattern Recognition (CVPR)*, pages 8344–8353, 2022.
- [15] Yu Sun, Xiaolong Wang, Zhuang Liu, John Miller, Alexei A. Efros, and Moritz Hardt. Test-time training with self-supervision for generalization under distribution shifts. In *International Conference on Machine Learning (ICML)*, 2020.
- [16] David Osowiechi, Gustavo A. Vargas Hakim, Mehrdad Noori, Milad Cheraghalikhani, Ismail Ayed, and Christian Desrosiers. Tttflow: Unsupervised test-time training with normalizing flow. In *2023 IEEE/CVF Winter Conference on Applications of Computer Vision (WACV)*, pages 2125–2126, Los Alamitos, CA, USA, jan 2023. IEEE Computer Society.
- [17] Yossi Gandelsman, Yu Sun, Xinlei Chen, and Alexei A Efros. Test-time training with masked autoencoders. In Alice H. Oh, Alekh Agarwal, Danielle Belgrave, and Kyunghyun Cho, editors, *Advances in Neural Information Processing Systems*, 2022.
- [18] Gustavo A Vargas Hakim, David Osowiechi, Mehrdad Noori, Milad Cheraghalikhani, Ali Bahri, Ismail Ben Ayed, and Christian Desrosiers. Clust3: Information invariant test-time training. In *Proceedings of the IEEE/CVF International Conference on Computer Vision*, pages 6136–6145, 2023.
- [19] David Osowiechi, Gustavo A. Vargas Hakim Hakim, Mehrdad Noori, Milad Cheraghalikhani, Ali Bahri, Moslem Yazdanpanah, Ismail Ben Ayed, and Christian Desrosiers. NC-TTT: A Noise Contrastive Approach for Test-Time Training, April 2024. arXiv:2404.08392 [cs].
- [20] Gustavo Adolfo Vargas Hakim, David Osowiechi, Mehrdad Noori, Milad Cheraghalikhani, Ali Bahri, Moslem Yazdanpanah, Ismail Ben Ayed, and Christian Desrosiers. Clipartt: Light-weight adaptation of clip to new domains at test time. *arXiv preprint arXiv:2405.00754*, 2024.
- [21] Xiaosong Ma, Jie ZHANG, Song Guo, and Wenchao Xu. Swapprompt: Test-time prompt adaptation for vision-language models. In *Thirty-seventh Conference on Neural Information Processing Systems*, 2023.
- [22] Pavel Izmailov, Dmitrii Podoprikin, Timur Garipov, Dmitry Vetrov, and Andrew Gordon Wilson. Averaging weights leads to wider optima and better generalization. *arXiv preprint arXiv:1803.05407*, 2018.
- [23] Geoffrey E Hinton and Sam Roweis. Stochastic neighbor embedding. *Advances in neural information processing systems*, 15, 2002.
- [24] Dan Hendrycks and Thomas Dietterich. Benchmarking neural network robustness to common corruptions and perturbations. *arXiv preprint arXiv:1903.12261*, 2019.
- [25] Xingchao Peng, Ben Usman, Neela Kaushik, Dequan Wang, Judy Hoffman, and Kate Saenko. Visda: A synthetic-to-real benchmark for visual domain adaptation. In *Proceedings of the IEEE Conference on Computer Vision and Pattern Recognition (CVPR) Workshops*, June 2018.
- [26] Da Li, Yongxin Yang, Yi-Zhe Song, and Timothy M Hospedales. Deeper, broader and artier domain generalization. In *Proceedings of the IEEE international conference on computer vision*, pages 5542–5550, 2017.
- [27] Chen Fang, Ye Xu, and Daniel N Rockmore. Unbiased metric learning: On the utilization of multiple datasets and web images for softening bias. In *Proceedings of the IEEE International Conference on Computer Vision*, pages 1657–1664, 2013.
- [28] Hemanth Venkateswara, Jose Eusebio, Shayok Chakraborty, and Sethuraman Panchanathan. Deep hashing network for unsupervised domain adaptation. In *Proceedings of the IEEE Conference on Computer Vision and Pattern Recognition*, pages 5018–5027, 2017.

# WATT: Weight Average Test-Time Adaption of CLIP

## Supplementary Material

### A Implementation

Our proposed WATT method is implemented in Python using the PyTorch (version 2.0.1) framework. All experiments were conducted on an NVIDIA V100 32 GB GPU. However, due to the efficiency and lightweight nature of our method, it can be executed on less powerful GPUs. Specifically, the adaptation with a batch size of 128 using the ViT/B32 backbone requires up to 4 GB of memory, making it feasible to use on a wide range of GPUs. For fairness and consistency, we re-implemented and ran all other methods, including CLIPArTT, TENT, and TPT, in the same environment. Each experiment was performed three times to ensure reliability (three trials per experiment). To facilitate reproducibility, we provide the original implementation and detailed step-by-step instructions in our anonymized repository, accessible via [this link](#).

### B Pseudo-code of our both methods

In Algorithms 1 and 2, we compare the two variants of WATT: one with Parallel MTWA (WATT-P) and the other with Sequential MTWA (WATT-S). The WATT-P model recalibrates its parameters for each template using the average parameters of  $m - 1$ , whereas the WATT-S model updates its parameters solely at the start of each new iteration  $m$ .

---

#### Algorithm 1 WATT-P - model $f$ , parameter $\theta$

---

```

1: for  $m \in \{1, 2, \dots, M\}$  do
2:    $\theta_{\text{avg}} \leftarrow \frac{1}{H} \sum_{h=1}^H \theta_h$ 
3:   for  $h \in \{1, 2, \dots, H\}$  do
4:      $f \leftarrow f_{\theta_{\text{avg}}}$ 
5:     for  $l \in \{1, 2, \dots, L\}$  do
6:        $\theta_h \leftarrow \mathcal{L}_{\text{TTA}}(f_{\theta_{\text{avg}}}(\text{template}_h))$ 
7:     end for
8:   end for
9: end for
```

---



---

#### Algorithm 2 WATT-S - model $f$ , parameter $\theta$

---

```

1: for  $m \in \{1, 2, \dots, M\}$  do
2:    $\theta_{\text{avg}} \leftarrow \frac{1}{H} \sum_{h=1}^H \theta_h$ 
3:    $f \leftarrow f_{\theta_{\text{avg}}}$ 
4:   for  $h \in \{1, 2, \dots, H\}$  do
5:     for  $l \in \{1, 2, \dots, L\}$  do
6:        $\theta_h \leftarrow \mathcal{L}_{\text{TTA}}(f_{\theta_{\text{avg}}}(\text{template}_h))$ 
7:     end for
8:   end for
9: end for
```

---

### C Additional Ablation Studies

**Cross Entropy vs Entropy minimization.** Two unsupervised loss functions were integrated into previous TTA methods: classical entropy minimization and the loss introduced by CLIPArTT [20], where predictions are utilized as pseudo-labels for cross-entropy computation. In Table 8, a comparison between these two loss functions is presented across the original CIFAR-10 dataset and various corruptions from CIFAR-10-C. It is observed that, for these specific corruptions, entropy minimization generally outperforms with the different templates employed, except for *Gaussian Noise*. However, upon assessing the weighted average accuracy, computed after 10 iterations for each template, cross-entropy consistently emerges as the superior option. The marginal impact of the weighted average on entropy minimization suggests that, irrespective of the template used, the model updates in a consistent direction to enhance confidence, rendering cross-entropy the preferred choice for subsequent experiments.

Dataset	Loss	$T^0$	$T^1$	$T^2$	$T^3$	$T^4$	$T^5$	$T^6$	$T^7$	WA
CIFAR-10	TENT	91.69	91.97	91.69	90.28	91.16	92.11	91.98	89.14	90.60
	CE	89.8	90.37	90.5	88.42	89.93	89.95	90.13	88.54	<b>91.05</b>
Gaussian Noise	TENT	41.27	37.16	46.39	51.31	39.27	32.51	49.7	42.96	47.08
	CE	60.19	61.01	61.17	58.24	58.84	58.35	59.62	61.13	<b>63.84</b>
Defocus Blur	TENT	77.12	77.13	78.7	76.09	76.85	76.59	77.86	74.31	76.21
	CE	77.23	77.07	78	75.98	76.39	77.45	77.08	75.59	<b>78.94</b>
Snow	TENT	78.29	79.54	80.09	75.39	78.97	78.52	78.78	75.82	77.24
	CE	76.57	77.36	77.93	75.08	77.45	77.09	77.05	75.57	<b>79.79</b>
JPEG Compression	TENT	62.64	65.83	64.27	59.49	62.78	64.19	62.62	63.39	65.31
	CE	64.65	65.36	65.24	64.16	64.18	64.36	64.78	65.32	<b>67.36</b>

Table 8: Comparison of accuracy (%) using entropy minimization (TENT) or cross-entropy (CE) on CIFAR-10 and some corruptions of CIFAR-10-C datasets with ViT-B/32 encoder on different templates (please see Table 2) and the weight average.

## D Experiments on other Visual Encoders

We replicated the experiments from the main paper using alternative visual encoders, ViT-B/16 and ViT-L/14.

Dataset	Backbone	CLIP	TENT	TPT (BS=32)	CLIPArTT	WATT-P	WATT-S
CIFAR-10	ViT-B/16	89.25	<b>92.75</b> $\pm 0.17$	89.80 $\pm 0.05$	92.61 $\pm 0.05$	92.31 $\pm 0.10$	91.97 $\pm 0.03$
	ViT-L/14	95.36	<b>96.13</b> $\pm 0.01$	95.18 $\pm 0.02$	95.16 $\pm 0.03$	95.91 $\pm 0.10$	95.71 $\pm 0.03$
CIFAR-10.1	ViT-B/16	84.00	88.52 $\pm 0.33$	83.75 $\pm 0.21$	<b>88.72</b> $\pm 0.33$	87.90 $\pm 0.11$	88.10 $\pm 0.08$
	ViT-L/14	91.20	92.22 $\pm 0.25$	91.32 $\pm 0.12$	91.02 $\pm 0.02$	<b>92.97</b> $\pm 0.13$	92.10 $\pm 0.33$
CIFAR-10-C	ViT-B/16	60.15	68.00	59.75	73.22	75.04	<b>76.22</b>
	ViT-L/14	76.04	79.18	75.01	78.06	80.05	<b>80.06</b>
CIFAR-100	ViT-B/16	64.76	71.73 $\pm 0.14$	67.15 $\pm 0.23$	71.34 $\pm 0.07$	<b>72.98</b> $\pm 0.07$	72.85 $\pm 0.15$
	ViT-L/14	73.28	78.03 $\pm 0.08$	76.85 $\pm 0.06$	<b>79.42</b> $\pm 0.08$	79.33 $\pm 0.05$	78.85 $\pm 0.19$
CIFAR-100-C	ViT-B/16	32.01	37.90	33.73	40.08	47.86	<b>48.95</b>
	ViT-L/14	44.59	50.14	47.58	52.52	54.10	<b>54.34</b>

Table 9: Accuracy (%) on CIFAR-10, CIFAR-10.1, CIFAR-10-C, CIFAR-100 and CIFAR-100-C datasets with ViT-B/16 and ViT-L/14 as visual encoders.

**Performance Evaluation in the Presence of Natural or No Domain Shift** As indicated in the main results, employing WATT, both with Parallel and Sequential MTWA, consistently enhances performance alongside the baseline. This pattern persists across different visual encoders, as shown in Tables 9. Although WATT consistently outperforms the baseline and TPT, TENT and CLIPArTT may occasionally yield superior results depending on the visual encoder used.

**Performance Evaluation in the Presence of Common Corruptions** Table 9 demonstrates a consistent trend where both WATT methods consistently outperform alternative methods across various corruptions and class numbers. Upon closer examination of Table 9, specifically with ViT-B/16 as the visual encoder, Sequential MTWA exhibits a significant performance advantage, surpassing the baseline by 16.07% and the leading method in the *state-of-the-art* by 3.00%. This trend becomes even more pronounced with an increased number of classes, where Sequential MTWA surpasses the baseline and CLIPArTT by 16.94% and 8.87%, respectively.

**Performance analysis under simulated and video shifts** Our study reveals substantial accuracy improvements on the 3D (simulated shift) and YT (video shift) partitions of VisDA-C when employing different backbones. This enhancement is particularly notable with our proposed WATT method compared to pure CLIP. Notably, the WATT-S variant achieves the highest accuracy across both

the 3D and YT partitions, outperforming various adaptation approaches including TENT, TPT, and CLIPArTT. Detailed comparisons can be found in Tables 10 and 11.

**Performance analysis under texture and style shifts** Findings across the OfficeHome, PACS, and VLCS datasets are detailed in Tables 10 and 11. Across these varied domains, our WATT method demonstrates consistent performance enhancements, as evidenced by both its WATT-P and WATT-S variants. These improvements underscore the efficacy of our approach in mitigating the complexities of texture and style shifts, which pose particular challenges compared to other forms of domain shift.

Dataset	Domain	CLIP	TENT	TPT	CLIPArTT	WATT-P	WATT-S
VisDA-C	3D (trainset)	87.16	87.57 $\pm 0.01$	84.04 $\pm 0.03$	87.58 $\pm 0.00$	87.61 $\pm 0.01$	<b>87.72 <math>\pm 0.02</math></b>
	YT (valset)	86.61	<b>86.81 <math>\pm 0.00</math></b>	85.90 $\pm 0.11$	86.60 $\pm 0.01$	86.66 $\pm 0.00$	86.75 $\pm 0.04$
	Mean	86.89	87.19	84.97	87.09	87.14	<b>87.24</b>
OfficeHome	Art	79.30	79.26 $\pm 0.14$	<b>81.97 <math>\pm 0.17</math></b>	79.34 $\pm 0.05$	80.37 $\pm 0.25$	80.43 $\pm 0.09$
	Clipart	65.15	65.64 $\pm 0.05$	67.01 $\pm 0.21$	65.69 $\pm 0.11$	<b>68.59 <math>\pm 0.13</math></b>	68.26 $\pm 0.11$
	Product	87.34	87.49 $\pm 0.02$	<b>89.00 <math>\pm 0.06</math></b>	87.35 $\pm 0.07$	88.15 $\pm 0.07$	88.02 $\pm 0.08$
	Real World	89.31	89.50 $\pm 0.04$	89.66 $\pm 0.06$	89.29 $\pm 0.03$	<b>90.18 <math>\pm 0.03</math></b>	90.14 $\pm 0.06$
	Mean	80.28	80.47	<b>81.91</b>	80.42	81.82	81.71
PACS	Art	97.44	97.54 $\pm 0.02$	95.10 $\pm 0.41$	97.64 $\pm 0.02$	97.49 $\pm 0.08$	<b>97.66 <math>\pm 0.08</math></b>
	Cartoon	97.38	97.37 $\pm 0.04$	91.42 $\pm 0.22$	97.37 $\pm 0.02$	97.47 $\pm 0.04$	<b>97.51 <math>\pm 0.02</math></b>
	Photo	<b>99.58</b>	<b>99.58 <math>\pm 0.00</math></b>	98.56 $\pm 0.40$	<b>99.58 <math>\pm 0.00</math></b>	<b>99.58 <math>\pm 0.00</math></b>	<b>99.58 <math>\pm 0.00</math></b>
	Sketch	86.06	86.37 $\pm 0.05$	87.23 $\pm 0.06$	86.79 $\pm 0.04$	<b>89.73 <math>\pm 0.16</math></b>	89.56 $\pm 0.14$
	Mean	95.12	95.22	93.08	95.35	96.07	<b>96.08</b>
VLCS	Caltech101	<b>99.43</b>	<b>99.43 <math>\pm 0.00</math></b>	97.62 $\pm 0.12$	<b>99.43 <math>\pm 0.00</math></b>	99.36 $\pm 0.00$	99.36 $\pm 0.00$
	LabelMe	67.75	67.31 $\pm 0.14$	49.77 $\pm 0.03$	67.74 $\pm 0.10$	67.55 $\pm 0.39$	<b>68.59 <math>\pm 0.25</math></b>
	SUN09	71.74	71.57 $\pm 0.15$	71.56 $\pm 0.86$	71.67 $\pm 0.01$	74.75 $\pm 0.07$	<b>75.16 <math>\pm 0.12</math></b>
	VOC2007	84.90	<b>85.10 <math>\pm 0.11</math></b>	71.17 $\pm 0.70$	84.73 $\pm 0.08$	82.53 $\pm 0.10$	83.24 $\pm 0.05$
	Mean	80.96	80.85	72.53	80.89	81.05	<b>81.59</b>

Table 10: Accuracy (%) on different domains of VisDA-C, OfficeHome, PACS and VLCS datasets with ViT-B/16 as visual encoder.

Dataset	Domain	CLIP	TENT	TPT	CLIPArTT	WATT-S
VisDA-C	3D (trainset)	91.24	91.40 $\pm 0.01$	90.65 $\pm 0.00$	91.34 $\pm 0.00$	<b>91.71 <math>\pm 0.00</math></b>
	YT (valset)	85.62	85.77 $\pm 0.01$	85.41 $\pm 0.06$	85.61 $\pm 0.01$	<b>86.80 <math>\pm 0.01</math></b>
	Mean	88.43	88.59	88.03	88.48	<b>89.26</b>
OfficeHome	Art	82.47	82.61 $\pm 0.15$	<b>86.76 <math>\pm 0.26</math></b>	82.35 $\pm 0.19$	84.43 $\pm 0.20$
	Clipart	72.20	72.51 $\pm 0.03$	74.76 $\pm 0.07$	72.41 $\pm 0.06$	<b>75.43 <math>\pm 0.08</math></b>
	Product	90.94	90.97 $\pm 0.02$	<b>92.42 <math>\pm 0.07</math></b>	90.94 $\pm 0.06$	91.88 $\pm 0.05$
	Real World	92.72	92.75 $\pm 0.02$	92.95 $\pm 0.16$	92.63 $\pm 0.03$	<b>94.06 <math>\pm 0.02</math></b>
	Mean	84.58	84.71	86.72	84.58	86.45
PACS	Art	98.68	<b>98.83 <math>\pm 0.00</math></b>	94.82 $\pm 0.34$	98.76 $\pm 0.02$	98.68 $\pm 0.00$
	Cartoon	97.74	97.74 $\pm 0.00$	95.65 $\pm 0.19$	97.74 $\pm 0.00$	<b>97.90 <math>\pm 0.02</math></b>
	Photo	99.54	99.54 $\pm 0.03$	99.44 $\pm 0.03$	<b>99.54 <math>\pm 0.00</math></b>	<b>99.64 <math>\pm 0.00</math></b>
	Sketch	93.28	93.51 $\pm 0.04$	92.72 $\pm 0.15$	93.26 $\pm 0.02$	<b>93.80 <math>\pm 0.02</math></b>
	Mean	97.31	97.41	95.66	97.33	<b>97.51</b>
VLCS	Caltech101	99.43	99.43 $\pm 0.00$	97.86 $\pm 0.43$	99.43 $\pm 0.00$	<b>99.51 <math>\pm 0.00</math></b>
	LabelMe	69.22	69.07 $\pm 0.12$	52.54 $\pm 0.20$	<b>69.32 <math>\pm 0.15</math></b>	62.76 $\pm 0.13$
	SUN09	68.06	68.23 $\pm 0.03$	69.49 $\pm 0.32$	67.89 $\pm 0.07$	<b>72.21 <math>\pm 0.15</math></b>
	VOC2007	83.99	84.08 $\pm 0.15$	76.16 $\pm 0.63$	<b>83.89 <math>\pm 0.13</math></b>	83.02 $\pm 0.12$
	Mean	80.18	<b>80.20</b>	74.01	80.13	79.38

Table 11: Accuracy (%) on different domains of VisDA-C, OfficeHome, PACS and VLCS datasets with ViT-L/14 as visual encoder.

## E Detailed Experimental Findings

This section provides extensive tables with detailed information on the results, which were summarized in the main body of the paper.

Dataset	single_temp	text_avg
CIFAR-10	90.87 $\pm$ 0.10	<b>91.08 <math>\pm</math>0.06</b>
CIFAR-10.1	86.80 $\pm$ 0.19	<b>86.85 <math>\pm</math>0.18</b>
CIFAR-10-C	Gaussian Noise	61.20 $\pm$ 0.05 <b>62.09 <math>\pm</math>0.15</b>
	Shot noise	63.16 $\pm$ 0.09 <b>63.51 <math>\pm</math>0.03</b>
	Impulse Noise	55.29 $\pm$ 0.22 <b>56.04 <math>\pm</math>0.16</b>
	Defocus blur	78.03 $\pm$ 0.12 <b>78.66 <math>\pm</math>0.07</b>
	Glass blur	62.7 $\pm$ 0.24 <b>63.35 <math>\pm</math>0.25</b>
	Motion blur	76.33 $\pm$ 0.11 <b>76.96 <math>\pm</math>0.14</b>
	Zoom blur	78.29 $\pm$ 0.05 <b>79.08 <math>\pm</math>0.15</b>
	Snow	78.65 $\pm$ 0.21 <b>78.95 <math>\pm</math>0.05</b>
	Frost	79.49 $\pm$ 0.11 <b>79.95 <math>\pm</math>0.06</b>
	Fog	77.21 $\pm$ 0.03 <b>77.72 <math>\pm</math>0.09</b>
	Brightness	86.60 $\pm$ 0.07 <b>86.98 <math>\pm</math>0.06</b>
	Contrast	79.22 $\pm$ 0.01 <b>79.62 <math>\pm</math>0.04</b>
	Elastic transform	71.17 $\pm$ 0.25 <b>71.61 <math>\pm</math>0.09</b>
	Pixelate	67.59 $\pm$ 0.08 <b>68.70 <math>\pm</math>0.15</b>
	JPEG compression	66.26 $\pm$ 0.00 <b>66.72 <math>\pm</math>0.01</b>
Mean	72.08	<b>72.66</b>

Table 12: Accuracy (%) on CIFAR-10, CIFAR-10.1 and CIFAR-10-C datasets with different text ensemble at test time. (WA after 10 iter) $\times$ 1

Dataset	single_temp	text_avg
CIFAR-100	69.79 $\pm$ 0.20	<b>70.30 <math>\pm</math>0.11</b>
CIFAR-100-C	Gaussian Noise	27.17 $\pm$ 0.22 <b>28.08 <math>\pm</math>0.21</b>
	Shot noise	29.69 $\pm$ 0.20 <b>30.47 <math>\pm</math>0.19</b>
	Impulse Noise	25.28 $\pm$ 0.10 <b>26.37 <math>\pm</math>0.28</b>
	Defocus blur	49.83 $\pm$ 0.11 <b>50.52 <math>\pm</math>0.04</b>
	Glass blur	27.83 $\pm$ 0.03 <b>28.25 <math>\pm</math>0.06</b>
	Motion blur	47.77 $\pm$ 0.21 <b>47.89 <math>\pm</math>0.21</b>
	Zoom blur	52.90 $\pm$ 0.16 <b>53.05 <math>\pm</math>0.10</b>
	Snow	50.31 $\pm$ 0.03 <b>50.22 <math>\pm</math>0.17</b>
	Frost	50.79 $\pm$ 0.07 <b>51.08 <math>\pm</math>0.09</b>
	Fog	48.70 $\pm$ 0.16 <b>48.48 <math>\pm</math>0.21</b>
	Brightness	61.22 $\pm$ 0.06 <b>61.56 <math>\pm</math>0.16</b>
	Contrast	47.87 $\pm$ 0.17 <b>47.90 <math>\pm</math>0.14</b>
	Elastic transform	37.55 $\pm$ 0.13 <b>37.93 <math>\pm</math>0.19</b>
	Pixelate	33.81 $\pm$ 0.06 <b>34.56 <math>\pm</math>0.14</b>
	JPEG compression	36.09 $\pm$ 0.13 <b>37.30 <math>\pm</math>0.18</b>
Mean	41.79	<b>42.24</b>

Table 13: Accuracy (%) on CIFAR-100 and CIFAR-100-C datasets with different text ensemble at test time. (WA after 10 iter) $\times$ 1

Dataset	Text avg.	Output avg.	Weight avg. (ours)		
			(after 10 iter) $\times$ 1	(after 1 iter) $\times$ 10	(after 2 iter) $\times$ 5
CIFAR-100	69.46 $\pm$ 0.13	70.32 $\pm$ 0.10	70.3 $\pm$ 0.11	<b>70.85 <math>\pm</math>0.08</b>	70.74 $\pm$ 0.20
CIFAR-100-C	Gaussian Noise	27.67 $\pm$ 0.11 28.58 $\pm$ 0.04	28.08 $\pm$ 0.21	31.67 $\pm$ 0.10	<b>32.07 <math>\pm</math>0.23</b>
	Shot noise	30.18 $\pm$ 0.06 31.05 $\pm$ 0.13	30.47 $\pm$ 0.19	34.26 $\pm$ 0.28	<b>34.36 <math>\pm</math>0.11</b>
	Impulse Noise	25.79 $\pm$ 0.02 26.86 $\pm$ 0.07	26.37 $\pm$ 0.28	30.12 $\pm$ 0.12	<b>30.33 <math>\pm</math>0.03</b>
	Defocus blur	49.51 $\pm$ 0.04 51.04 $\pm$ 0.02	50.52 $\pm$ 0.04	52.76 $\pm$ 0.25	<b>52.99 <math>\pm</math>0.16</b>
	Glass blur	27.88 $\pm$ 0.22 28.72 $\pm$ 0.08	28.25 $\pm$ 0.06	31.95 $\pm$ 0.08	<b>32.15 <math>\pm</math>0.30</b>
	Motion blur	46.68 $\pm$ 0.05 48.30 $\pm$ 0.19	47.89 $\pm$ 0.21	50.46 $\pm$ 0.10	<b>50.53 <math>\pm</math>0.12</b>
	Zoom blur	52.05 $\pm$ 0.07 53.72 $\pm$ 0.11	53.05 $\pm$ 0.10	55.13 $\pm$ 0.29	<b>55.30 <math>\pm</math>0.22</b>
	Snow	49.40 $\pm$ 0.18 51.01 $\pm$ 0.13	50.22 $\pm$ 0.17	52.60 $\pm$ 0.26	<b>52.77 <math>\pm</math>0.15</b>
	Frost	49.68 $\pm$ 0.04 51.50 $\pm$ 0.06	51.08 $\pm$ 0.09	53.30 $\pm$ 0.21	<b>53.79 <math>\pm</math>0.31</b>
	Fog	47.36 $\pm$ 0.17 48.67 $\pm$ 0.22	48.48 $\pm$ 0.21	51.35 $\pm$ 0.08	<b>51.49 <math>\pm</math>0.21</b>
	Brightness	60.42 $\pm$ 0.12 61.74 $\pm$ 0.31	61.56 $\pm$ 0.16	63.23 $\pm$ 0.12	<b>63.57 <math>\pm</math>0.21</b>
	Contrast	46.86 $\pm$ 0.05 48.14 $\pm$ 0.10	47.90 $\pm$ 0.14	52.40 $\pm$ 0.23	<b>52.76 <math>\pm</math>0.27</b>
	Elastic transform	37.00 $\pm$ 0.37 38.55 $\pm$ 0.23	37.93 $\pm$ 0.19	40.97 $\pm$ 0.11	<b>40.90 <math>\pm</math>0.43</b>
	Pixelate	33.65 $\pm$ 0.12 34.63 $\pm$ 0.17	34.56 $\pm$ 0.14	40.32 $\pm$ 0.08	<b>40.97 <math>\pm</math>0.16</b>
	JPEG compression	36.38 $\pm$ 0.11 37.67 $\pm$ 0.23	37.30 $\pm$ 0.18	39.35 $\pm$ 0.19	<b>39.59 <math>\pm</math>0.08</b>
Mean	41.37	42.68	42.24	45.32	<b>45.57</b>

Table 14: Accuracy (%) on CIFAR-100 and CIFAR-100-C datasets with different averaging

Dataset	Text avg.	Output avg.	Weight avg. (ours)			
			(after 10 iter)×1	(after 1 iter)×10	(after 2 iter)×5	
CIFAR-10	90.58 ±0.03	90.90 ±0.03	91.08 ±0.06	<b>91.39 ±0.14</b>	91.05 ±0.06	
CIFAR-10.1	85.78 ±0.25	86.77 ±0.08	86.85 ±0.18	<b>88.02 ±0.18</b>	86.98 ±0.31	
CIFAR-10-C	Gaussian Noise	61.23 ±0.13	62.22 ±0.12	62.09 ±0.15	63.42 ±0.07	<b>63.84 ±0.24</b>
	Shot noise	62.88 ±0.15	63.98 ±0.17	63.51 ±0.03	64.93 ±0.13	<b>65.28 ±0.21</b>
	Impulse Noise	54.71 ±0.07	56.41 ±0.11	56.04 ±0.16	58.37 ±0.37	<b>58.64 ±0.11</b>
	Defocus blur	77.93 ±0.12	78.63 ±0.18	78.66 ±0.07	<b>79.11 ±0.17</b>	78.94 ±0.12
	Glass blur	62.37 ±0.18	63.32 ±0.07	63.35 ±0.25	64.67 ±0.18	<b>65.12 ±0.07</b>
	Motion blur	75.55 ±0.19	76.97 ±0.05	76.96 ±0.14	77.56 ±0.12	<b>77.81 ±0.14</b>
	Zoom blur	77.86 ±0.06	78.90 ±0.18	79.08 ±0.15	<b>79.76 ±0.03</b>	79.32 ±0.07
	Snow	77.77 ±0.03	78.92 ±0.03	78.95 ±0.05	<b>79.89 ±0.26</b>	79.79 ±0.06
	Frost	78.51 ±0.09	79.67 ±0.09	79.95 ±0.06	80.52 ±0.04	<b>80.54 ±0.12</b>
	Fog	76.04 ±0.17	77.54 ±0.10	77.72 ±0.09	78.44 ±0.21	<b>78.53 ±0.22</b>
	Brightness	86.08 ±0.13	86.75 ±0.04	86.98 ±0.06	<b>87.32 ±0.14</b>	87.11 ±0.11
	Contrast	77.87 ±0.02	79.48 ±0.07	79.62 ±0.04	80.77 ±0.35	<b>81.20 ±0.22</b>
	Elastic transform	69.98 ±0.16	71.20 ±0.22	71.61 ±0.09	72.52 ±0.19	<b>72.66 ±0.15</b>
	Pixelate	66.78 ±0.29	68.27 ±0.17	68.70 ±0.15	70.50 ±0.20	<b>71.11 ±0.13</b>
	JPEG compression	65.62 ±0.28	66.78 ±0.08	66.72 ±0.01	67.05 ±0.10	<b>67.36 ±0.28</b>
Mean	71.41	72.60	72.66	73.66	<b>73.82</b>	

Table 15: Accuracy (%) on CIFAR-10, CIFAR-10.1 and CIFAR-10-C datasets with different averaging

Dataset	CLIP	BS = 1	BS = 2	BS = 4	BS = 8	BS = 16	BS = 32	BS = 64	BS = 128	
CIFAR-10	88.74	89.87	89.39 $\pm 0.02$	89.16 $\pm 0.07$	88.93 $\pm 0.16$	89.14 $\pm 0.04$	89.51 $\pm 0.12$	90.16 $\pm 0.13$	91.05 $\pm 0.06$	
CIFAR-10.1	83.25	84.55	84.32 $\pm 0.15$	83.88 $\pm 0.17$	84.12 $\pm 0.37$	84.35 $\pm 0.21$	84.87 $\pm 0.16$	85.52 $\pm 0.30$	86.98 $\pm 0.31$	
CIFAR-10-C	Gaussian Noise	35.27	38.55	43.85 $\pm 0.26$	45.41 $\pm 0.10$	47.95 $\pm 0.15$	51.79 $\pm 0.27$	56.35 $\pm 0.11$	60.87 $\pm 0.33$	63.84 $\pm 0.24$
	Shot noise	39.67	42.57	46.87 $\pm 0.25$	47.95 $\pm 0.15$	49.13 $\pm 0.14$	52.57 $\pm 0.03$	56.96 $\pm 0.10$	61.84 $\pm 0.06$	65.28 $\pm 0.21$
	Impulse Noise	42.61	42.92	47.94 $\pm 0.29$	48.20 $\pm 0.18$	48.69 $\pm 0.11$	50.53 $\pm 0.18$	53.32 $\pm 0.19$	55.81 $\pm 0.11$	58.64 $\pm 0.11$
	Defocus blur	69.76	72.29	72.80 $\pm 0.13$	72.95 $\pm 0.13$	72.57 $\pm 0.20$	73.71 $\pm 0.18$	75.28 $\pm 0.18$	77.37 $\pm 0.08$	78.94 $\pm 0.12$
	Glass blur	42.40	44.15	48.15 $\pm 0.15$	47.69 $\pm 0.07$	48.96 $\pm 0.04$	52.59 $\pm 0.19$	57.83 $\pm 0.24$	62.16 $\pm 0.20$	65.12 $\pm 0.07$
	Motion blur	63.97	66.37	67.53 $\pm 0.07$	67.22 $\pm 0.01$	68.00 $\pm 0.12$	69.20 $\pm 0.11$	71.60 $\pm 0.06$	74.75 $\pm 0.09$	77.81 $\pm 0.14$
	Zoom blur	69.83	71.50	72.60 $\pm 0.14$	72.30 $\pm 0.04$	72.39 $\pm 0.01$	73.19 $\pm 0.06$	75.01 $\pm 0.09$	77.03 $\pm 0.27$	79.32 $\pm 0.07$
	Snow	71.78	73.72	74.46 $\pm 0.16$	73.97 $\pm 0.19$	74.12 $\pm 0.05$	74.62 $\pm 0.22$	76.06 $\pm 0.06$	77.64 $\pm 0.06$	79.79 $\pm 0.06$
	Frost	72.86	75.67	76.50 $\pm 0.23$	75.98 $\pm 0.11$	75.55 $\pm 0.16$	76.32 $\pm 0.13$	77.67 $\pm 0.03$	78.82 $\pm 0.20$	80.54 $\pm 0.12$
	Fog	67.04	68.88	70.25 $\pm 0.02$	69.94 $\pm 0.06$	69.88 $\pm 0.09$	71.02 $\pm 0.15$	73.10 $\pm 0.02$	75.95 $\pm 0.04$	78.53 $\pm 0.22$
	Brightness	81.87	83.52	83.73 $\pm 0.10$	83.38 $\pm 0.03$	83.31 $\pm 0.05$	83.51 $\pm 0.11$	84.49 $\pm 0.13$	85.40 $\pm 0.07$	87.11 $\pm 0.11$
	Contrast	64.37	67.02	69.67 $\pm 0.13$	68.64 $\pm 0.14$	69.08 $\pm 0.06$	71.11 $\pm 0.17$	74.58 $\pm 0.14$	78.25 $\pm 0.22$	81.20 $\pm 0.22$
	Elastic transf.	60.83	62.04	64.25 $\pm 0.13$	63.50 $\pm 0.40$	63.46 $\pm 0.10$	64.65 $\pm 0.28$	66.63 $\pm 0.21$	69.58 $\pm 0.18$	72.66 $\pm 0.15$
	Pixelate	50.53	51.65	55.18 $\pm 0.26$	55.47 $\pm 0.14$	56.30 $\pm 0.29$	58.88 $\pm 0.21$	63.00 $\pm 0.08$	67.43 $\pm 0.11$	71.11 $\pm 0.13$
	JPEG compr.	55.48	58.12	60.17 $\pm 0.04$	59.44 $\pm 0.18$	59.74 $\pm 0.04$	61.20 $\pm 0.09$	63.15 $\pm 0.15$	65.32 $\pm 0.16$	67.36 $\pm 0.28$
Mean	59.22	61.26	63.60	63.47	63.94	65.66	68.34	71.21	73.82	

Table 16: Accuracy (%) on CIFAR-10, CIFAR-10.1 and CIFAR-10-C datasets with ViT-B/16 as visual encoder for different number of batches.



Dataset	T=1	T=2	T=4	T=6	T=8	
CIFAR-10	89.42 $\pm$ 0.84	90.74 $\pm$ 0.30	90.98 $\pm$ 0.14	91.34 $\pm$ 0.16	91.05 $\pm$ 0.06	
CIFAR-10.1	85.08 $\pm$ 0.59	86.49 $\pm$ 0.59	87.20 $\pm$ 0.48	87.53 $\pm$ 0.21	86.98 $\pm$ 0.31	
CIFAR-10-C	Gaussian Noise	59.82 $\pm$ 1.43	62.05 $\pm$ 0.62	62.79 $\pm$ 0.18	63.49 $\pm$ 0.27	63.84 $\pm$ 0.24
	Shot noise	62.32 $\pm$ 1.32	63.35 $\pm$ 0.43	64.73 $\pm$ 0.31	65.02 $\pm$ 0.10	65.28 $\pm$ 0.21
	Impulse Noise	54.07 $\pm$ 0.17	56.83 $\pm$ 0.33	57.53 $\pm$ 0.47	58.37 $\pm$ 0.08	58.64 $\pm$ 0.11
	Defocus blur	77.09 $\pm$ 0.24	78.32 $\pm$ 0.32	78.92 $\pm$ 0.16	79.17 $\pm$ 0.26	78.94 $\pm$ 0.12
	Glass blur	60.64 $\pm$ 0.29	63.77 $\pm$ 0.43	64.42 $\pm$ 0.68	64.64 $\pm$ 0.39	65.12 $\pm$ 0.07
	Motion blur	74.60 $\pm$ 0.50	77.02 $\pm$ 0.32	77.70 $\pm$ 0.26	77.73 $\pm$ 0.12	77.81 $\pm$ 0.14
	Zoom blur	77.40 $\pm$ 0.29	78.93 $\pm$ 0.46	79.28 $\pm$ 0.54	79.33 $\pm$ 0.24	79.32 $\pm$ 0.07
	Snow	76.96 $\pm$ 1.04	78.83 $\pm$ 0.31	79.47 $\pm$ 0.29	79.69 $\pm$ 0.33	79.79 $\pm$ 0.06
	Frost	77.62 $\pm$ 0.86	79.27 $\pm$ 0.45	80.04 $\pm$ 0.26	80.46 $\pm$ 0.17	80.54 $\pm$ 0.12
	Fog	75.32 $\pm$ 0.57	77.27 $\pm$ 0.39	78.00 $\pm$ 0.17	78.55 $\pm$ 0.29	78.53 $\pm$ 0.22
	Brightness	85.13 $\pm$ 0.58	86.74 $\pm$ 0.22	87.07 $\pm$ 0.20	87.13 $\pm$ 0.21	87.11 $\pm$ 0.11
	Contrast	77.18 $\pm$ 0.68	79.74 $\pm$ 0.31	80.32 $\pm$ 0.07	80.69 $\pm$ 0.12	81.20 $\pm$ 0.22
	Elastic transform	69.39 $\pm$ 0.39	71.40 $\pm$ 0.24	72.25 $\pm$ 0.14	72.28 $\pm$ 0.34	72.66 $\pm$ 0.15
	Pixelate	66.26 $\pm$ 0.76	68.86 $\pm$ 0.68	69.47 $\pm$ 0.39	71.00 $\pm$ 0.57	71.11 $\pm$ 0.13
	JPEG compression	64.58 $\pm$ 0.58	66.28 $\pm$ 0.14	66.82 $\pm$ 0.24	67.16 $\pm$ 0.18	67.36 $\pm$ 0.28
Mean	70.56	72.58	73.25	73.65	73.82	

Table 17: Accuracy (%) on CIFAR-10, CIFAR-10.1 and CIFAR-10-C datasets with ViT-B/16 as visual encoder for different number of templates randomly picked over 5 runs.

Dataset		CLIP	TENT	TPT (BS=32)	CLIPArTT	WATT-P	WATT-S
CIFAR-10		88.74	<b>91.69</b> $\pm$ 0.10	88.06 $\pm$ 0.06	90.04 $\pm$ 0.13	91.41 $\pm$ 0.17	91.05 $\pm$ 0.06
CIFAR-10.1		83.25	87.60 $\pm$ 0.45	81.80 $\pm$ 0.27	86.35 $\pm$ 0.27	<b>87.78</b> $\pm$ 0.05	86.98 $\pm$ 0.31
CIFAR-10-C	Gaussian Noise	35.27	41.27 $\pm$ 0.27	33.90 $\pm$ 0.08	59.90 $\pm$ 0.36	61.89 $\pm$ 0.24	<b>63.84</b> $\pm$ 0.24
	Shot noise	39.67	47.20 $\pm$ 0.23	38.20 $\pm$ 0.02	62.77 $\pm$ 0.07	63.52 $\pm$ 0.08	<b>65.28</b> $\pm$ 0.21
	Impulse Noise	42.61	48.58 $\pm$ 0.31	37.66 $\pm$ 0.20	56.02 $\pm$ 0.16	57.13 $\pm$ 0.02	<b>58.64</b> $\pm$ 0.11
	Defocus blur	69.76	77.12 $\pm$ 0.16	67.83 $\pm$ 0.28	76.74 $\pm$ 0.05	78.86 $\pm$ 0.09	<b>78.94</b> $\pm$ 0.12
	Glass blur	42.40	52.65 $\pm$ 0.30	38.81 $\pm$ 0.12	61.77 $\pm$ 0.16	62.88 $\pm$ 0.06	<b>65.12</b> $\pm$ 0.07
	Motion blur	63.97	71.25 $\pm$ 0.09	63.39 $\pm$ 0.13	76.01 $\pm$ 0.19	76.85 $\pm$ 0.26	<b>77.81</b> $\pm$ 0.14
	Zoom blur	69.83	76.20 $\pm$ 0.19	68.95 $\pm$ 0.16	77.40 $\pm$ 0.20	<b>79.35</b> $\pm$ 0.04	79.32 $\pm$ 0.07
	Snow	71.78	78.29 $\pm$ 0.20	70.16 $\pm$ 0.10	77.29 $\pm$ 0.16	79.44 $\pm$ 0.09	<b>79.79</b> $\pm$ 0.06
	Frost	72.86	79.84 $\pm$ 0.09	72.39 $\pm$ 0.22	79.20 $\pm$ 0.08	80.13 $\pm$ 0.10	<b>80.54</b> $\pm$ 0.12
	Fog	67.04	77.39 $\pm$ 0.01	64.31 $\pm$ 0.28	75.74 $\pm$ 0.14	77.68 $\pm$ 0.07	<b>78.53</b> $\pm$ 0.22
	Brightness	81.87	<b>87.78</b> $\pm$ 0.03	81.30 $\pm$ 0.18	86.59 $\pm$ 0.16	87.10 $\pm$ 0.10	87.11 $\pm$ 0.11
	Contrast	64.37	79.47 $\pm$ 0.11	62.26 $\pm$ 0.31	77.82 $\pm$ 0.14	80.04 $\pm$ 0.24	<b>81.20</b> $\pm$ 0.22
	Elastic transform	60.83	70.00 $\pm$ 0.25	56.43 $\pm$ 0.27	70.20 $\pm$ 0.01	71.76 $\pm$ 0.10	<b>72.66</b> $\pm$ 0.15
	Pixelate	50.53	63.74 $\pm$ 0.18	42.80 $\pm$ 0.40	66.52 $\pm$ 0.13	69.28 $\pm$ 0.09	<b>71.11</b> $\pm$ 0.13
	JPEG compression	55.48	62.64 $\pm$ 0.14	53.67 $\pm$ 0.25	63.51 $\pm$ 0.14	66.49 $\pm$ 0.14	<b>67.36</b> $\pm$ 0.28
Mean		59.22	67.56	56.80	71.17	72.83	<b>73.82</b>

Table 18: Accuracy (%) on CIFAR-10, CIFAR-10.1 and CIFAR-10-C datasets with ViT-B/32 as visual encoder.

Dataset	CLIP	TENT	TPT (BS=32)	CLIPArTT	WATT-P	WATT-S
CIFAR-10	89.25	92.75 $\pm 0.17$	89.80 $\pm 0.05$	92.61 $\pm 0.05$	92.31 $\pm 0.10$	91.97 $\pm 0.03$
CIFAR-10.1	84.00	88.52 $\pm 0.33$	83.75 $\pm 0.21$	88.72 $\pm 0.33$	87.9 $\pm 0.11$	88.10 $\pm 0.08$
CIFAR-10-C	Gaussian Noise	37.75	31.04 $\pm 0.38$	35.35 $\pm 0.15$	60.89 $\pm 0.26$	63.10 $\pm 0.12$
	Shot noise	41.10	40.54 $\pm 0.41$	41.03 $\pm 0.19$	65.19 $\pm 0.21$	66.31 $\pm 0.10$
	Impulse Noise	51.71	58.03 $\pm 0.16$	54.86 $\pm 0.07$	67.55 $\pm 0.09$	69.62 $\pm 0.12$
	Defocus blur	70.07	77.57 $\pm 0.03$	70.29 $\pm 0.02$	78.92 $\pm 0.12$	79.64 $\pm 0.08$
	Glass blur	42.24	47.16 $\pm 0.05$	37.86 $\pm 0.17$	57.18 $\pm 0.20$	58.98 $\pm 0.12$
	Motion blur	65.81	76.16 $\pm 0.05$	67.43 $\pm 0.11$	76.59 $\pm 0.06$	78.32 $\pm 0.16$
	Zoom blur	72.50	79.64 $\pm 0.12$	72.91 $\pm 0.02$	79.62 $\pm 0.11$	80.67 $\pm 0.07$
	Snow	73.23	81.68 $\pm 0.03$	72.98 $\pm 0.32$	81.13 $\pm 0.29$	81.99 $\pm 0.10$
	Frost	76.52	83.22 $\pm 0.05$	75.87 $\pm 0.16$	81.24 $\pm 0.08$	83.41 $\pm 0.16$
	Fog	68.35	80.78 $\pm 0.15$	69.13 $\pm 0.27$	78.47 $\pm 0.19$	81.36 $\pm 0.12$
	Brightness	83.36	89.85 $\pm 0.11$	83.67 $\pm 0.14$	88.66 $\pm 0.15$	89.06 $\pm 0.05$
	Contrast	61.90	79.24 $\pm 0.19$	62.16 $\pm 0.06$	75.15 $\pm 0.07$	81.57 $\pm 0.23$
	Elastic transform	53.16	62.54 $\pm 0.08$	51.26 $\pm 0.23$	69.49 $\pm 0.08$	69.14 $\pm 0.09$
	Pixelate	48.48	67.08 $\pm 0.24$	44.65 $\pm 0.21$	71.80 $\pm 0.16$	73.38 $\pm 0.29$
	JPEG compression	56.05	65.42 $\pm 0.05$	56.73 $\pm 0.07$	66.42 $\pm 0.25$	69.02 $\pm 0.10$
Mean	60.15	68.00	59.75	73.22	75.04	76.22

Table 19: Accuracy (%) on CIFAR-10, CIFAR-10.1 and CIFAR-10-C datasets with ViT-B/16 as visual encoder.

Dataset	CLIP	TENT	TPT (BS=32)	CLIPArTT	WATT-P	WATT-S
CIFAR-100	64.76	71.73 $\pm 0.14$	67.15 $\pm 0.23$	71.34 $\pm 0.07$	72.98 $\pm 0.07$	72.85 $\pm 0.15$
CIFAR-100-C	Gaussian Noise	15.88	12.28 $\pm 0.20$	15.43 $\pm 0.03$	19.01 $\pm 0.24$	34.23 $\pm 0.03$
	Shot noise	17.49	15.07 $\pm 0.21$	16.88 $\pm 0.07$	20.27 $\pm 0.21$	36.68 $\pm 0.1$
	Impulse Noise	21.43	13.13 $\pm 0.16$	22.12 $\pm 0.15$	17.66 $\pm 0.10$	43.17 $\pm 0.35$
	Defocus blur	40.10	50.35 $\pm 0.03$	41.08 $\pm 0.22$	49.86 $\pm 0.13$	53.13 $\pm 0.12$
	Glass blur	13.48	4.84 $\pm 0.14$	18.43 $\pm 0.15$	18.34 $\pm 0.31$	32.53 $\pm 0.03$
	Motion blur	39.82	49.85 $\pm 0.37$	40.85 $\pm 0.26$	50.00 $\pm 0.09$	51.63 $\pm 0.06$
	Zoom blur	45.45	54.76 $\pm 0.04$	46.77 $\pm 0.06$	54.13 $\pm 0.08$	56.81 $\pm 0.11$
	Snow	42.77	52.38 $\pm 0.18$	47.24 $\pm 0.18$	52.80 $\pm 0.27$	56.04 $\pm 0.06$
	Frost	45.39	51.66 $\pm 0.04$	48.61 $\pm 0.14$	49.56 $\pm 0.08$	56.00 $\pm 0.11$
	Fog	38.98	50.74 $\pm 0.14$	39.92 $\pm 0.16$	49.92 $\pm 0.11$	52.88 $\pm 0.33$
	Brightness	52.55	64.26 $\pm 0.09$	55.83 $\pm 0.10$	63.76 $\pm 0.13$	65.58 $\pm 0.07$
	Contrast	33.32	48.69 $\pm 0.08$	33.13 $\pm 0.16$	47.86 $\pm 0.02$	52.90 $\pm 0.06$
	Elastic transform	24.39	33.56 $\pm 0.28$	27.36 $\pm 0.10$	32.93 $\pm 0.23$	39.82 $\pm 0.21$
	Pixelate	21.89	36.20 $\pm 0.28$	21.26 $\pm 0.10$	39.49 $\pm 0.21$	45.10 $\pm 0.06$
	JPEG compression	27.21	30.80 $\pm 0.05$	30.97 $\pm 0.10$	35.56 $\pm 0.23$	41.43 $\pm 0.18$
Mean	32.01	37.90	33.73	40.08	47.86	48.95

Table 20: Accuracy (%) on CIFAR-100 and CIFAR-100-C datasets with ViT-B/16 as visual encoder.

Dataset		CLIP	TENT	TPT (BS=32)	CLIPArTT	WATT-P	WATT-S
CIFAR-10		95.36	96.13 $\pm 0.06$	95.18 $\pm 0.02$	95.16 $\pm 0.03$	95.91 $\pm 0.10$	95.71 $\pm 0.03$
CIFAR-10.1		91.20	92.22 $\pm 0.25$	91.32 $\pm 0.12$	91.02 $\pm 0.02$	92.97 $\pm 0.13$	92.10 $\pm 0.33$
CIFAR-10-C	Gaussian Noise	64.64	68.87 $\pm 0.20$	64.44 $\pm 0.11$	70.04 $\pm 0.31$	72.81 $\pm 0.09$	72.73 $\pm 0.03$
	Shot noise	67.82	71.95 $\pm 0.06$	66.81 $\pm 0.19$	71.44 $\pm 0.16$	74.45 $\pm 0.16$	74.60 $\pm 0.03$
	Impulse Noise	78.21	80.22 $\pm 0.19$	76.46 $\pm 0.17$	79.42 $\pm 0.15$	81.36 $\pm 0.09$	80.95 $\pm 0.15$
	Defocus blur	80.73	83.10 $\pm 0.03$	79.01 $\pm 0.23$	81.75 $\pm 0.19$	83.20 $\pm 0.10$	83.15 $\pm 0.18$
	Glass blur	50.29	57.12 $\pm 0.07$	49.64 $\pm 0.23$	58.13 $\pm 0.23$	61.51 $\pm 0.07$	62.35 $\pm 0.15$
	Motion blur	80.75	82.69 $\pm 0.11$	78.85 $\pm 0.04$	80.76 $\pm 0.12$	82.60 $\pm 0.13$	82.61 $\pm 0.12$
	Zoom blur	82.75	84.91 $\pm 0.08$	82.32 $\pm 0.13$	83.39 $\pm 0.05$	85.76 $\pm 0.06$	85.44 $\pm 0.13$
	Snow	83.01	85.99 $\pm 0.11$	82.69 $\pm 0.10$	84.48 $\pm 0.07$	84.91 $\pm 0.13$	85.61 $\pm 0.15$
	Frost	84.90	87.15 $\pm 0.12$	84.63 $\pm 0.08$	85.21 $\pm 0.06$	87.17 $\pm 0.13$	86.88 $\pm 0.04$
	Fog	78.44	81.30 $\pm 0.07$	77.56 $\pm 0.17$	79.27 $\pm 0.07$	81.80 $\pm 0.11$	81.79 $\pm 0.09$
	Brightness	91.67	93.07 $\pm 0.04$	90.94 $\pm 0.04$	91.87 $\pm 0.09$	92.78 $\pm 0.05$	92.59 $\pm 0.16$
	Contrast	84.20	87.93 $\pm 0.04$	82.88 $\pm 0.09$	86.19 $\pm 0.06$	87.54 $\pm 0.12$	87.38 $\pm 0.02$
	Elastic transform	65.45	69.96 $\pm 0.12$	64.81 $\pm 0.14$	67.43 $\pm 0.24$	71.19 $\pm 0.07$	71.25 $\pm 0.09$
	Pixelate	75.10	77.89 $\pm 0.05$	72.92 $\pm 0.12$	77.11 $\pm 0.10$	77.88 $\pm 0.13$	77.67 $\pm 0.16$
	JPEG compression	72.58	75.49 $\pm 0.07$	71.18 $\pm 0.19$	74.46 $\pm 0.11$	75.88 $\pm 0.16$	75.84 $\pm 0.18$
Mean		76.04	79.18	75.01	78.06	80.05	80.06

Table 21: Accuracy (%) on CIFAR-10, CIFAR-10.1 and CIFAR-10-C datasets with ViT-L/14 as visual encoder.

Dataset	CLIP	TENT	TPT <sub>(BS=32)</sub>	CLIPArTT	WATT-P	WATT-S	
CIFAR-100	73.28	78.03 $\pm 0.08$	76.85 $\pm 0.06$	79.42 $\pm 0.08$	79.33 $\pm 0.05$	78.85 $\pm 0.19$	
CIFAR-100-C	Gaussian Noise	30.55	36.93 $\pm 0.03$	36.10 $\pm 0.11$	41.46 $\pm 0.15$	43.99 $\pm 0.13$	44.13 $\pm 0.11$
	Shot noise	34.58	40.96 $\pm 0.16$	38.23 $\pm 0.13$	44.27 $\pm 0.09$	46.28 $\pm 0.22$	46.63 $\pm 0.17$
	Impulse Noise	44.89	49.09 $\pm 0.14$	49.69 $\pm 0.21$	51.44 $\pm 0.23$	56.15 $\pm 0.04$	56.26 $\pm 0.22$
	Defocus blur	48.88	55.23 $\pm 0.07$	50.43 $\pm 0.19$	56.55 $\pm 0.22$	57.46 $\pm 0.01$	57.66 $\pm 0.42$
	Glass blur	23.46	27.02 $\pm 0.23$	24.35 $\pm 0.22$	30.47 $\pm 0.14$	32.54 $\pm 0.12$	33.54 $\pm 0.16$
	Motion blur	50.83	56.03 $\pm 0.20$	51.94 $\pm 0.04$	56.98 $\pm 0.18$	58.22 $\pm 0.10$	57.81 $\pm 0.05$
	Zoom blur	56.02	61.19 $\pm 0.10$	56.96 $\pm 0.16$	62.56 $\pm 0.04$	62.94 $\pm 0.02$	62.74 $\pm 0.06$
	Snow	49.03	55.60 $\pm 0.09$	54.89 $\pm 0.11$	58.81 $\pm 0.11$	60.68 $\pm 0.06$	61.04 $\pm 0.27$
	Frost	53.27	58.21 $\pm 0.15$	58.15 $\pm 0.33$	60.38 $\pm 0.23$	62.34 $\pm 0.14$	62.76 $\pm 0.22$
	Fog	48.51	53.37 $\pm 0.25$	49.26 $\pm 0.13$	54.38 $\pm 0.04$	54.71 $\pm 0.31$	54.70 $\pm 0.13$
	Brightness	60.53	67.34 $\pm 0.17$	66.60 $\pm 0.10$	69.63 $\pm 0.14$	71.52 $\pm 0.07$	71.60 $\pm 0.09$
	Contrast	50.24	59.91 $\pm 0.13$	53.64 $\pm 0.24$	63.39 $\pm 0.13$	62.77 $\pm 0.22$	63.95 $\pm 0.04$
	Elastic transform	35.07	38.49 $\pm 0.12$	35.72 $\pm 0.09$	39.57 $\pm 0.39$	41.28 $\pm 0.25$	41.27 $\pm 0.15$
	Pixelate	43.86	48.37 $\pm 0.17$	44.32 $\pm 0.10$	50.45 $\pm 0.16$	51.15 $\pm 0.15$	51.22 $\pm 0.13$
	JPEG compression	39.11	44.42 $\pm 0.09$	43.44 $\pm 0.11$	47.45 $\pm 0.14$	49.40 $\pm 0.17$	49.78 $\pm 0.18$
Mean	44.59	50.14	47.58	52.52	54.10	54.34	

Table 22: Accuracy (%) on CIFAR-100 and CIFAR-100-C datasets with ViT-L/14 as visual encoder.